

# Simultaneous probing of geometry and electronic orbital of ArCO by Coulomb-explosion imaging and angle-dependent tunneling rates

X. Gong,<sup>1</sup> M. Kunitski,<sup>2</sup> L. Ph. H. Schmidt,<sup>2</sup> T. Jahnke,<sup>2</sup> A. Czasch,<sup>2</sup> R. Dörner,<sup>2</sup> and J. Wu<sup>1,\*</sup>

<sup>1</sup>*State Key Laboratory of Precision Spectroscopy, East China Normal University, Shanghai 200062, China*

<sup>2</sup>*Institut für Kernphysik, Goethe Universität, Max-von-Laue-Strasse 1, D-60438 Frankfurt, Germany*

(Received 21 May 2013; published 25 July 2013)

We simultaneously probe the molecular structure and the symmetry of valence electronic orbital of an anisotropic atomic-molecular complex of ArCO by tracing its three-body Coulomb breakup following triple ionization in a phase-controlled elliptically polarized two-color pulse. The geometry of ArCO is found to be tilted T shaped, where the angle between the covalent and van der Waals bonds is  $65^\circ$  with oxygen pointing towards argon. The asymmetric profiles of the outmost orbitals from the CO site are probed by directional dissociation of the contained CO subunit as a function of the laser phase. Our results clearly image the asymmetric geometry of ArCO and thus reveal the anisotropic interaction between a rare-gas atom and a heteronuclear diatomic molecule.

DOI: [10.1103/PhysRevA.88.013422](https://doi.org/10.1103/PhysRevA.88.013422)

PACS number(s): 33.80.Rv, 42.50.Hz, 42.65.Re

## I. INTRODUCTION

The intermolecular force is significant in both forming matter in the condensed phase by holding individual molecules together and guiding chemical reactions of approaching molecules. The study of the van der Waals (vdW) complex composed of a rare-gas atom and a heteronuclear diatomic molecule leads to the fundamental understanding of the anisotropic intermolecular interaction. To that end, a primary step is the knowledge of the molecular geometry and the electronic orbital of the anisotropic atom-molecule complex, which is also crucial to understand its physical and chemical properties as well as the interaction potential-energy surface.

The molecular geometry can be probed by using the x-ray diffraction [1], rotational and vibrational spectroscopies [2–4], Coulomb explosion imaging [5–8], the laser-driven electron recollision or diffraction [9–11], or it can be predicted by quantum chemical calculations [12–14]. Most intuitively the Coulomb explosion of the multiply charged molecular ion following the sudden stripping of several electrons directly images the molecular geometry. On the other hand, the molecular orbital can be probed by using the molecular-orientation-dependent ionization rate [15,16] or by scanning tunneling microscopy [17]. The angular dependence of strong-field ionization rates is predicted, for example, by molecular Ammosov-Delone-Krainov (MO-ADK) theory [18]. Experimentally phase-controlled few-cycle [19,20] or two-color laser pulses [21–24] have been used as tools to study the orientation dependence of the strong-field ionization rate.

In this paper, we use these recently developed strong-field tools to probe the anisotropic atomic-molecular vdW complex ArCO for which even the structure is not known exactly [3,13,14]. We break the complex by triple ionization in a phase-controlled elliptically polarized two-color pulse and image both the Coulomb explosion which gives us the molecular geometry and the directional fragmentation which reveals the orbital symmetry. It serves as a prototype system for the investigation of the anisotropic intermolecular interaction [14,25,26] and has been studied for many decades since

its experimental observation [2]. Most of the effort is to determine its geometry and the interaction potential-energy surface [27]. Both the infrared or microwave spectroscopy measurements [3,4] and the associated quantum chemical simulations [12–14] indicate an approximately T-shaped configuration of ArCO. However, not even for the bond angle between the covalent and vdW bonds has a consensus been achieved. Various bond angles ranging from  $49^\circ$  to  $117^\circ$  [3,12–14,26,27] have been anticipated for ArCO, which was even proposed to be very floppy [9,14,27]. Here, we image the geometry of ArCO by exploding the complex in an intense laser field, and find a bond angle of  $65^\circ$  with oxygen pointing towards argon. The symmetry of the ionizing orbitals at the CO site is simultaneously probed by tracing the laser phase-dependent directional dissociation of the contained CO subunit. Our results directly show the anisotropic intermolecular interaction between a rare-gas atom and a heteronuclear diatomic molecule. It meanwhile provides a benchmark for quantum calculations and is significant to refine the potential-energy surface calculations.

## II. EXPERIMENTAL SETUP

We performed the experiments in a cold target recoil ion momentum spectroscopy (COLTRIMS) reaction microscope [28], where the fragment ions from a laser induced multiple ionization of the ArCO complex were measured in coincidence. The triple-ionization-induced three-body breakup channel  $\text{ArCO} \rightarrow \text{Ar}^+ + \text{C}^+ + \text{O}^+ + 3e$ , which we will refer to as ArCO(1,1,1), was used for simultaneous probing of the molecular geometry and orbital. The phase-controlled elliptically polarized two-color pulse was generated in a collinear scheme driven by a linearly polarized femtosecond laser pulse from a Ti:sapphire laser system (35 fs, 790 nm, 8 kHz) as detailed in Ref. [24], which was used to simultaneously probe the geometry and orbital of ArCO. In other words, probing both geometry and orbital asymmetry of ArCO complex has been performed in a single measurement under the same experimental conditions. By using a concave mirror ( $f = 7.5$  cm) inside the chamber, the laser pulse was focused onto a supersonic beam where ArCO was generated

\*jwu@phy.ecnu.edu.cn

by coexpanding a gas mixture of CO and Ar through a 30- $\mu\text{m}$  nozzle. The intensities of the fundamental-wave (FW) and second-harmonic (SH) components in the interaction region were estimated to be  $7.6 \times 10^{14}$  and  $3.4 \times 10^{14}$  W/cm<sup>2</sup>, respectively.

### III. GEOMETRY PROBING

As illustrated in Fig. 1, we measure the angle  $\angle_{(\text{Ar},\text{CO}),\text{mea}}$  between the final momenta but we aim at determining the bond angle  $\angle_{(\text{Ar},\text{CO})}$  between the bond axes. To obtain the bond angle, we first identify those events where the fragmentation is direct and not sequential with intermediate rotation of metastable fragments, and second we use a molecular-dynamics simulation to retrieve the bond angle from the final momenta. We calculate the angle  $\angle_{(\text{Ar},\text{CO}),\text{mea}} = \cos^{-1} [(\mathbf{p}_{\text{rel}(\text{O}^+, \text{C}^+)} \cdot \mathbf{p}_{\text{Ar}^+}) / (|\mathbf{p}_{\text{rel}(\text{O}^+, \text{C}^+)}| |\mathbf{p}_{\text{Ar}^+}|)]$ , where  $\mathbf{p}_{\text{rel}(\text{O}^+, \text{C}^+)} = 0.5(\mathbf{p}_{\text{O}^+} - \mathbf{p}_{\text{C}^+}) + 0.5\mathbf{p}_{\text{Ar}^+}(m_{\text{C}} - m_{\text{O}})/(m_{\text{C}} + m_{\text{O}})$  is the relative momentum between C<sup>+</sup> to O<sup>+</sup>. The observed ArCO(1,1,1) channel can be created through either direct explosion after sudden stripping of three electrons at the equilibrium configuration or sequentially by first creating Ar<sup>+</sup> and a metastable CO<sup>2+</sup> in the laser pulse and then the intermediate CO<sup>2+</sup> dissociates later into C<sup>+</sup> and O<sup>+</sup>. As previously demonstrated in Refs. [29,30], the post-pulse dissociation of the intermediate molecular ion usually concurs with its rotation which smears out the initial orientation of the molecular bonds. Therefore, to retrieve the equilibrium bond angle  $\angle_{(\text{Ar},\text{CO})}$  of the complex, the ArCO(1,1,1) events of direct three-body breakup must be discriminated from the sequential process.

As shown in Fig. 2(a), the direct (labeled as region *D*) and sequential (labeled as region *S*) processes can be clearly separated in the kinetic-energy-release (KER) distribution of Ar<sup>+</sup>,  $\text{KER}_{\text{Ar}^+} = 0.5|\mathbf{p}_{\text{Ar}^+}|^2/m_{\text{Ar}}$ , as a function of the exploding

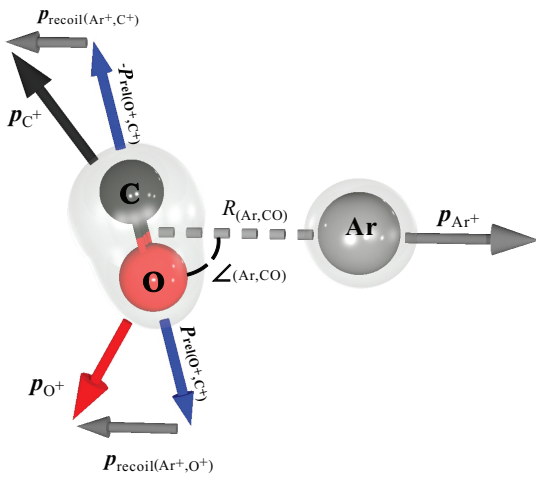


FIG. 1. (Color online) Schematic illustration of the geometry and orbital (transparent blobs) of the ArCO complex.  $\angle_{(\text{Ar},\text{CO})}$ : the bond angle between the covalent and van der Waals bonds;  $R_{(\text{Ar},\text{CO})}$ : the distance between Ar and the center of mass of CO;  $\mathbf{p}_{\text{Ar}^+}$ ,  $\mathbf{p}_{\text{C}^+}$ , and  $\mathbf{p}_{\text{O}^+}$ : the momenta of Ar<sup>+</sup>, C<sup>+</sup>, and O<sup>+</sup> ions;  $\mathbf{p}_{\text{rel}(\text{O}^+, \text{C}^+)}$ : the relative momentum between C<sup>+</sup> and O<sup>+</sup>;  $\mathbf{p}_{\text{recoil}(\text{Ar}^+, \text{C}^+)}$  and  $\mathbf{p}_{\text{recoil}(\text{Ar}^+, \text{O}^+)}$ : the recoil momenta on C<sup>+</sup> and O<sup>+</sup> from departing Ar<sup>+</sup>.

KER of (C<sup>+</sup>,O<sup>+</sup>) pair,  $\text{KER}_{\text{C}^+, \text{O}^+} = 0.5|\mathbf{p}_{\text{rel}(\text{O}^+, \text{C}^+)}|^2(m_{\text{C}} + m_{\text{O}})/m_{\text{C}}m_{\text{O}}$ . For the sequential breakup, the Ar<sup>+</sup> receives a relatively larger  $\text{KER}_{\text{Ar}^+}$  in the first-step Ar<sup>+</sup>-CO<sup>2+</sup> as compared to the direct case where the positive point charges localize at the separated C<sup>+</sup> and O<sup>+</sup> rather than their center of mass. The higher  $\text{KER}_{(\text{C}^+, \text{O}^+)}$  for the events in region *D* from direct breakup as compared to those in region *S* from sequential process is consistent with the observations of the dissociation of CO<sup>2+</sup> following the *K*-shell photionization of CO monomer [29], where the direct dissociation from a steep repulsive potential curve through vertical population led to a high KER and the rotation accompanied stepwise dissociation resulted in a low KER of the (C<sup>+</sup>,O<sup>+</sup>) pair.

The ring structure (labeled with a red dashed circle) of the Newton diagram in Fig. 2(b) clearly maps the rotation of the long-lived intermediate CO<sup>2+</sup> before its dissociation in the sequential breakup process. In the Newton diagram, the magnitudes of the momenta of C<sup>+</sup>,  $\mathbf{p}'_{\text{C}^+} = \mathbf{p}_{\text{C}^+} + 0.5\mathbf{p}_{\text{Ar}^+}m_{\text{C}}/(m_{\text{C}} + m_{\text{O}})$ , and O<sup>+</sup>,  $\mathbf{p}'_{\text{O}^+} = \mathbf{p}_{\text{O}^+} + 0.5\mathbf{p}_{\text{Ar}^+}m_{\text{O}}/(m_{\text{C}} + m_{\text{O}})$ , are normalized to the magnitude of  $\mathbf{p}_{\text{Ar}^+}$  (labeled with an orange arrow) which points to the right with a length of unity. In the sequential breakup process, the Ar<sup>+</sup> departs from CO<sup>2+</sup> in the first step and is independent of the subsequent rotation and dissociation of CO<sup>2+</sup>. Its momentum  $\mathbf{p}_{\text{Ar}^+}$  or  $\text{KER}_{\text{Ar}^+}$  is governed by the Coulomb repulsion between the ion of the (Ar<sup>+</sup>, CO<sup>2+</sup>) pair produced in the first step and reflects the instantaneous distance between them at the ionization moment. It corresponds to a concentrated flat line in the Dalitz plot [31] as shown in Fig. 2(c), where the coordinates are defined as  $\epsilon_{\text{Ar}^+} = |\mathbf{p}_{\text{Ar}^+}|^2/|\mathbf{p}_{\text{sum}}|^2 - 1/3$ ,  $\epsilon_{(\text{C}^+, \text{O}^+)} = (|\mathbf{p}_{\text{O}^+}|^2 - |\mathbf{p}_{\text{C}^+}|^2)/\sqrt{3} \times |\mathbf{p}_{\text{sum}}|^2$ , and  $|\mathbf{p}_{\text{sum}}|^2 = |\mathbf{p}_{\text{Ar}^+}|^2 + |\mathbf{p}_{\text{C}^+}|^2 + |\mathbf{p}_{\text{O}^+}|^2$ . By assuming a pure Coulomb potential for repulsive interaction in the first-step generated (Ar<sup>+</sup>, CO<sup>2+</sup>) pair, the equilibrium distance from Ar to the center of mass of the CO subunit,  $R_{(\text{Ar},\text{CO})}$  as shown in Fig. 1, is classically estimated to be  $\sim 4.0$  Å based on the measured  $\text{KER}_{\text{Ar}^+} = 2.9$  eV from the sequential breakup.

One of our main interests is in the bond angle  $\angle_{(\text{Ar},\text{CO})}$ , which we now try to obtain from the direct breakup of ArCO(1,1,1) after sudden stripping of three electrons in its equilibrium configuration. As shown in Figs. 2(b) and 2(d), it corresponds to the concentrated distribution almost perpendicular to  $\mathbf{p}_{\text{Ar}^+}$  outside the sequential ring, according to a rapid explosion of (C<sup>+</sup>,O<sup>+</sup>) pair in the presence of Ar<sup>+</sup> in the direct breakup process. As shown in Fig. 2(d), the distribution of C<sup>+</sup> and O<sup>+</sup> are slightly tilted with O<sup>+</sup> being closer to Ar<sup>+</sup>, indicating an anisotropic intermolecular interaction between CO and Ar in forming the ArCO complex. This tilted distribution corresponds to an asymmetric distribution of the crossing angle  $\angle_{(\text{Ar},\text{CO}),\text{mea}}$  as shown in Fig. 3(a), whose statistical centroid is  $\angle_{(\text{Ar},\text{CO}),\text{mea}} = 86.4^\circ$ .

We note that the axial recoil approximation may not be satisfied for retrieving bond orientation for multibond breaking of polyatomic molecules. In the case of the vdW complex composed of a homonuclear diatomic molecule and a rare-gas atom, such as ArN<sub>2</sub>, the classical simulations show that the Coulomb repulsion of the fragment ions ends with an observed crossing angle tending to 90° even for an initialized bond angle that deviates from 90°. This deviation between the real bond

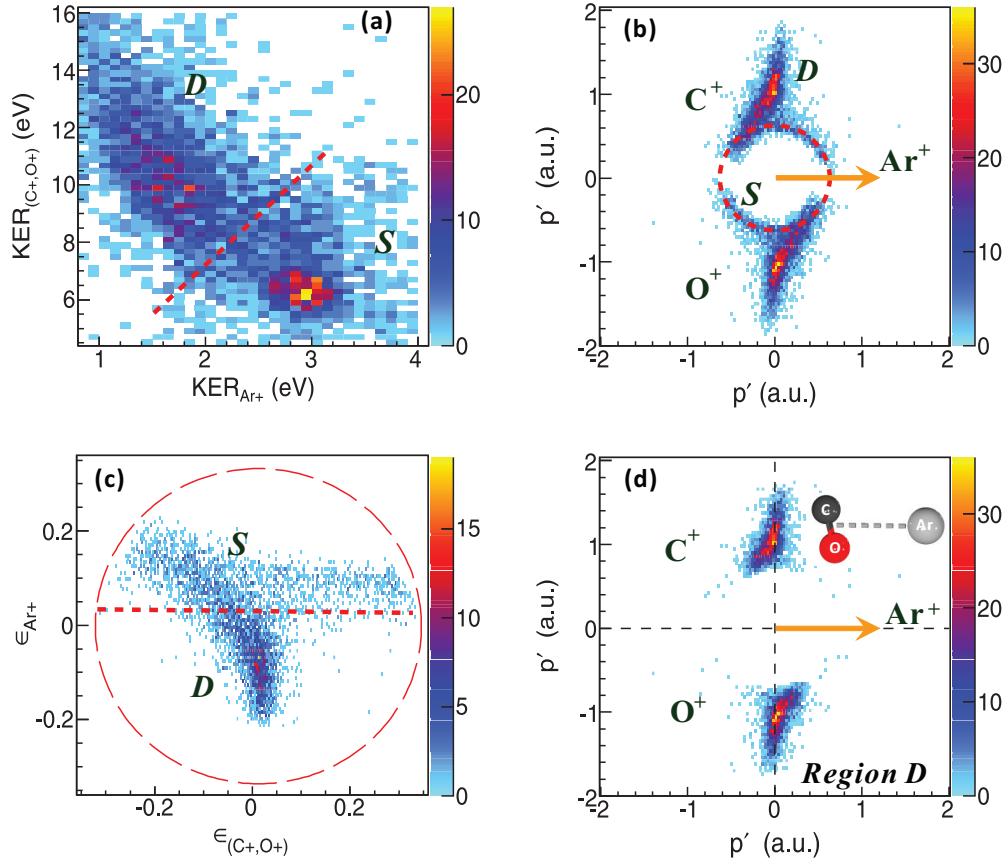


FIG. 2. (Color online) (a) Distribution of  $\text{KER}_{\text{Ar}^+}$  vs  $\text{KER}_{(\text{C}^+, \text{O}^+)}$  of the  $\text{ArCO}(1,1,1)$  channel, where the direct and sequential breakup processes are labeled  $D$  and  $S$ , respectively. (b) Newton diagram of the  $\text{ArCO}(1,1,1)$  channel. The magnitudes of the momenta of  $\mathbf{p}'_{\text{C}^+}$  and  $\mathbf{p}'_{\text{O}^+}$  are normalized to the magnitude of  $\mathbf{p}_{\text{Ar}^+}$  which points to the right with a length of unity as labeled with an orange arrow. (c) Dalitz plot of the  $\text{ArCO}(1,1,1)$  channel (see details in text). (d) The same as (b) but only the even regions from region  $D$ .

angle and the observed crossing angle becomes even stronger when an anisotropic interaction is involved, such as for  $\text{ArCO}$ . In general, the connection between the bond angle and the observed angle between the fragment momenta also depends on the detailed potential curve on which it dissociates. As demonstrated in Ref. [29],  $\text{CO}^{2+}$  with  $\text{KER}_{(\text{C}^+, \text{O}^+)}$  above 10.2 eV dissociates on the purely repulsive curve of  ${}^3\Sigma^-$  [32,33] for the events in the direct breakup region. This potential-energy curve deviates from the pure Coulomb potential curve  $1/R$  at short internuclear distance [see Fig. 3(b)]. We retrieved the initial bond angle from our measured final-state fragment momenta by an iterative initial configuration search algorithm based on a classical molecular-dynamics simulation of the fragmentation. In the optimization procedure we monitor the calculated total KER of the fragment ions,  $\text{KER}_{(\text{C}^+, \text{O}^+)}$ , and  $\text{KER}_{\text{Ar}^+}$  so that their mismatch from the experimental values is less than 1%. We perform our molecular-dynamics simulation with two alternative potentials for the  $\text{CO}^{2+}$ , the  ${}^3\Sigma^-$  potential curve which is known to govern the dissociation, and a  $1/R$  potential, which is not realistic for the  $\text{CO}^{2+}$  states most probably populated in our laser pulse, but which serves as the most extreme case for comparison. For the realistic  ${}^3\Sigma^-$  potential curve, the observed crossing angle  $\angle_{(\text{Ar}, \text{CO}), \text{mea}}$  of  $86.4^\circ$  corresponds to a real bond-angle  $\angle_{(\text{Ar}, \text{CO})}$  of  $65^\circ$  with  $R_{(\text{Ar}, \text{CO})} = 3.9 \text{ \AA}$  and  $R_{(\text{C}, \text{O})} = 1.27 \text{ \AA}$ . For the  $1/R$  potential we obtain a bond angle of  $57^\circ$  as indicated by the red dashed

line in Fig. 3(c). Both values lie in the range of the pioneering spectroscopy measurements [3,4,27] and quantum simulations [9–11]. We do not consider the latter value of  $57^\circ$  realistic and show it here only for comparison. With respect to the spectroscopic measurements [3,4], the coincidentally measured momenta of the fragment ions presented in this work clearly image the geometry of  $\text{ArCO}$ , which will help to refine the potential-energy surface calculation.

#### IV. ORBITAL PROBING

We now discuss the symmetry of the electronic orbitals and ask if the presence of Ar will change the axial symmetry of the outmost orbitals of CO in the  $\text{ArCO}$  complex. We address this question by tracing the laser phase-dependent directional emission of the  $(\text{C}^+, \text{O}^+)$  pair from the direct breakup of  $\text{ArCO}(1,1,1)$  and compare it to the CO molecule which is also present in our jet and hence measured simultaneously. As schematically shown in Fig. 1, bound by the weak vdW force, the orbitals of  $\text{ArCO}$  localize around the Ar and CO sites, which allow us to individually probe the orbitals of the contained CO subunit. In strong laser fields, the tunneling rate of the electron from atoms and molecules strongly depends on the ionization potential. Besides a few percent of vdW complex, most of the jet is composed of the Ar and CO monomers. Based on the measured ion yields of  $\text{Ar}^+$  and  $\text{CO}^+$

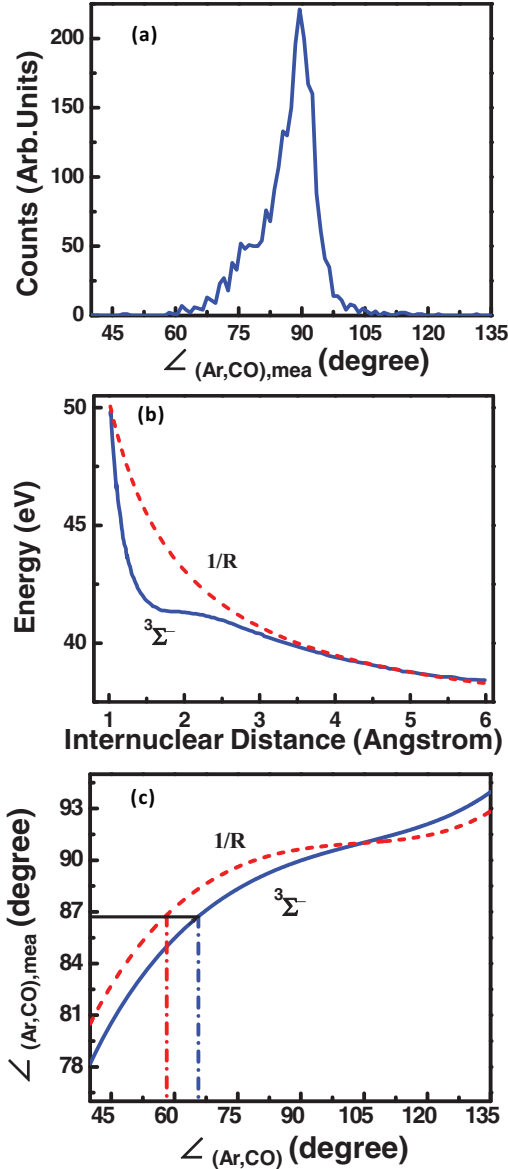


FIG. 3. (Color online) (a) The retrieved distributions of  $\angle_{(Ar,CO),mea}$  from the triple-ionization-induced direct breakup of ArCO. (b) The repulsive potential of  ${}^3\Sigma^-$  of  $CO^{2+}$  (adapted from Ref. [32]) and the Coulomb potential of  $1/R$ . (c) The  $\angle_{(Ar,CO),mea}$  as a function of  $\angle_{(Ar,CO)}$  simulated for the direct breakup ArCO(1,1,1) by assuming a potential curve of  ${}^3\Sigma^-$  or a Coulomb potential of  $1/R$  for the dissociation of  $CO^{2+}$ .

in the same experiment, we estimate that the single ionization probability of CO is about two orders of magnitude higher than that of Ar. It is in accord with the fact that the single ionization potential of CO ( $I_p \sim 14.0$  eV) is lower than that of Ar ( $I_p \sim 15.7$  eV). For ArCO, the first electron is hence most likely to be freed from the CO site rather than from Ar. The Ar site will most probably still be neutral at the time the CO subunit is ionized during the pulse and hence will not alter the CO ionization step.

We continuously vary the phase of the two-color laser pulse  $\phi$ , i.e., the difference between the FW and SH components, from 0 to  $\pi$  by scanning the insert thickness of a fused silica wedge pair in the beam line. The changing of  $\phi$

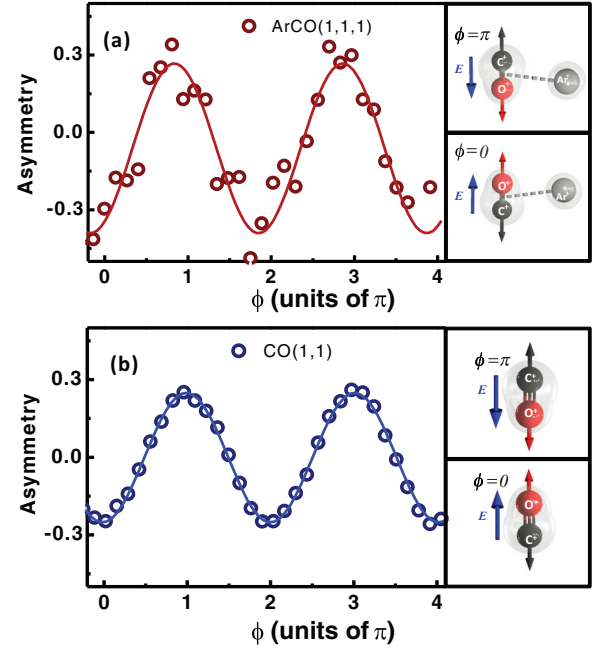


FIG. 4. (Color online) Phase-dependent directional emission of  $C^+$  from (a) the direct breakup channel of ArCO(1,1,1), and (b) the CO(1,1) channel following double ionization of CO monomer, measured within a  $45^\circ$  cone around  $y$  axis. The right panels schematically show the field-direction-dependent directional dissociation of ArCO and CO.

alters the field maximum of the elliptically polarized two-color pulse along its major axis (along  $y$  in our laboratory coordinate system), which points to  $+y$  and  $-y$  for  $\phi = 0$  and  $\pi$ , respectively. We accurately determine the phase  $\phi$  of the elliptically polarized two-color pulse by tracing the rotating-field streaked momentum of the released electron or its recoil on the correlated ion [24]. Figure 4(a) shows the phase-dependent asymmetric emission of  $C^+$ , i.e.,  $[p_{(C^+,+y)} - p_{(C^+,-y)}]/[p_{(C^+,+y)} + p_{(C^+,-y)}]$ , of the  $(C^+,O^+)$  pair from the direct breakup ArCO(1,1,1) within the polarization plane ( $45^\circ$  cone around the  $y$  axis). It shows almost the same phase dependence as the directional emission of  $C^+$  from the double ionization of CO monomer as shown in Fig. 4(b),  $CO \rightarrow C^+ + O^+ + 2e$ , which is labeled CO(1,1), measured simultaneously in the same experiment. It is ruled by the asymmetric profile of the ionizing orbital [34]. Our experiment shows that the symmetry of the outmost orbitals at the CO site of ArCO is very similar to that of the free CO molecule.

## V. CONCLUSIONS

In summary, by using phased-controlled elliptically polarized two-color femtosecond laser pulses, we have simultaneously probed the geometrical structure and the symmetry of valence orbital of an anisotropic polyatomic complex composed of a rare-gas atom and a heteronuclear diatomic molecule. Our results clearly imaged the tilted T-shaped geometry of the ArCO complex. Additionally, it has been found that argon has neglecting weak influence on the symmetry of the outmost CO orbital in this complex. Thus, the phase-controlled two-color pulse induced strong-field multiple ionization alternatively

provides an approach to simultaneously probe the geometry and orbital of polyatomic molecules.

#### ACKNOWLEDGMENTS

This work was supported by a Koselleck Project of the Deutsche Forschungsgemeinschaft, the Program for

Professor of Special Appointment (Eastern Scholar) at Shanghai Institutions of Higher Learning and for NCET in University (NCET-12-0177), the Projects from the Shanghai Science and Technology Commission (13QH1401400), the “Shu Guang” project (12SG25), and the Program of Introducing Talents of Discipline to Universities (B12024).

- 
- [1] A. O. Er, J. Chen, and P. M. Rentzepis, *J. Appl. Phys.* **112**, 031101 (2012).
- [2] A. De Piante, E. J. Campbell, and S. J. Buelow, *Rev. Sci. Instrum.* **60**, 858 (1989).
- [3] T. Ogata, W. Jäger, I. Ozier, and M. C. L. Gerry, *J. Chem. Phys.* **98**, 9399 (1993).
- [4] Y. Xu and A. R. W. Mckellar, *Mol. Phys.* **88**, 859 (1996).
- [5] U. Werner, K. Beckord, J. Becker, and H. O. Lutz, *Phys. Rev. Lett.* **74**, 1962 (1995).
- [6] C. Cornaggia, *Laser Phys.* **19**, 1660 (2009).
- [7] B. Ulrich, A. Vredenburg, A. Malakzadeh, L. Ph. H. Schmidt, T. Havermeier, M. Meckel, K. Cole, M. Smolarski, Z. Chang, T. Jahnke, and R. Dörner, *J. Phys. Chem. A* **115**, 6936 (2011).
- [8] J. Wu, M. Kunitski, L. Ph. H. Schmidt, T. Jahnke, and R. Dörner, *J. Chem. Phys.* **137**, 104308 (2012).
- [9] J. Itatani, J. Levesque, D. Zeidler, H. Niikura, H. Pépin, J. C. Kieffer, P. B. Corkum, and D. M. Villeneuve, *Nature (London)* **432**, 867 (2004).
- [10] M. Meckel, D. Comtois, D. Zeidler, A. Staudte, D. Pavičić, H. C. Bandulet, H. Pépin, J. C. Kieffer, R. Dörner, D. M. Villeneuve, and P. B. Corkum, *Science* **320**, 1478 (2008).
- [11] J. P. Marangos, S. Baker, J. S. Robinson, R. Torres, J. W. G. Tisch, C. C. Chirila, M. Lein, R. Velotta, and C. Altucci, *Strong Field Laser Phys.* **134**, 209 (2009).
- [12] V. Castells, N. Halberstadt, S. K. Shin, R. A. Beaudet, and C. Wittig, *J. Chem. Phys.* **101**, 1006 (1994).
- [13] B. Tarnawska, G. Chałasiński, and K. Olszewski, *J. Chem. Phys.* **101**, 4964 (1994).
- [14] G. Jansen, *J. Chem. Phys.* **105**, 89 (1996).
- [15] N. Saito, K. Ueda, A. D. Fanis, K. Kubozuka, M. Machida, I. Koyano, R. Dörner, A. Czasch, L. Schmidt, A. Cassimi, K. Wang, B. Zimmermann, and V. McKoy, *J. Phys. B* **38**, L277 (2005).
- [16] D. Pavičić, K. F. Lee, D. M. Rayner, P. B. Corkum, and D. M. Villeneuve, *Phys. Rev. Lett.* **98**, 243001 (2007).
- [17] J. I. Pascual, J. Gómez-Herrero, C. Rogero, A. M. Baró, D. Sánchez-Portal, E. Artacho, P. Ordejón, and J. M. Soler, *Chem. Phys. Lett.* **321**, 78 (2000).
- [18] X. M. Tong, Z. X. Zhao, and C. D. Lin, *Phys. Rev. A* **66**, 033402 (2002).
- [19] M. F. Kling, Ch. Siedschlag, A. J. Verhoef, J. I. Khan, M. Schultze, Th. Uphues, Y. Ni, M. Uiberacker, M. Drescher, F. Krausz, and M. J. J. Vrakking, *Science* **312**, 246 (2006).
- [20] I. Znakovskaya, P. von den Hoff, G. Marcus, S. Zherebtsov, B. Bergues, X. Gu, Y. Deng, M. J. J. Vrakking, R. Kienberger, F. Krausz, R. de Vivie-Riedle, and M. F. Kling, *Phys. Rev. Lett.* **108**, 063002 (2012).
- [21] H. Ohmura, N. Saito, and M. Tachiya, *Phys. Rev. Lett.* **96**, 173001 (2006).
- [22] K. J. Betsch, D. W. Pinkham, and R. R. Jones, *Phys. Rev. Lett.* **105**, 223002 (2010).
- [23] H. Li, D. Ray, S. De, I. Znakovskaya, W. Cao, G. Laurent, Z. Wang, M. F. Kling, A. T. Le, and C. L. Cocke, *Phys. Rev. A* **84**, 043429 (2011).
- [24] J. Wu, A. Vredenburg, L. Ph. H. Schmidt, T. Jahnke, A. Czasch, and R. Dörner, *Phys. Rev. A* **87**, 023406 (2013).
- [25] I. Scheele, R. Lehnig, and M. Havenith, *Mol. Phys.* **99**, 205 (2001).
- [26] F. A. Gianturco and F. Paesani, *J. Chem. Phys.* **115**, 249 (2001).
- [27] L. H. Coudert, I. Pak, and L. Surin, *J. Chem. Phys.* **121**, 4691 (2004).
- [28] R. Dörner, V. Mergel, O. Jagutzki, L. Spielberger, J. Ullrich, R. Moshhammer, and H. Schmidt-Böcking, *Phys. Rep.* **330**, 95 (2000).
- [29] T. Weber, O. Jagutzki, M. Hattass, A. Staudte, A. Nauert, L. Schmidt, M. H. Prior, A. L. Landers, A. Bräuning-Demian, H. Bräuning, C. L. Cocke, T. Osipov, I. Ali, R. D. Muiño, D. Rolles, F. J. García de Abajo, C. S. Fadley, M. A. VanHove, A. Cassimi, H. Schmidt-Böcking, and R. Dörner, *J. Phys. B* **34**, 3669 (2001).
- [30] N. Neumann, D. Hant, L. Ph. H. Schmidt, J. Titze, T. Jahnke, A. Czasch, M. S. Schöffler, K. Kreidi, O. Jagutzki, H. Schmidt-Böcking, and R. Dörner, *Phys. Rev. Lett.* **104**, 103201 (2010).
- [31] J. Laksman, D. Céolin, M. Gisselbrecht, and S. L. Sorensen, *J. Chem. Phys.* **133**, 144314 (2010).
- [32] J. H. D. Eland, M. Hochlaf, G. C. King, P. S. Kreymin, R. J. LeRoy, I. R. McNab, and J. M. Robbe, *J. Phys. B* **37**, 3197 (2004).
- [33] T. Šedivcová, P. R. Žďánská, and V. Špirko, *J. Chem. Phys.* **124**, 214303 (2006).
- [34] J. Wu, L. Ph. H. Schmidt, M. Kunitski, M. Meckel, S. Voss, H. Sann, H. Kim, T. Jahnke, A. Czasch, and R. Dörner, *Phys. Rev. Lett.* **108**, 183001 (2012).